

On an array localization technique with Euclidean distance geometry

Simon Bouley

Univ Lyon, INSA-Lyon, Laboratoire Vibrations Acoustique, F-69621 Villeurbanne, France

Charles Vanwynsberghe

Univ Lyon, INSA-Lyon, Laboratoire Vibrations Acoustique, F-69621 Villeurbanne, France

Thibaut Le Magueresse

MicrodB, 28 Chemin du Petit Bois, Écully, France

Jérôme Antoni

Univ Lyon, INSA-Lyon, Laboratoire Vibrations Acoustique, F-69621 Villeurbanne, France

Summary

The localization of sources by an acoustic array of microphones depends to a great extent on an accurate knowledge of the antenna position in its environment. From the geometric data of the array and the object of study, the present work details a methodology to determine the location of the microphones in relation to the object and reproduce the experimental configuration. Reference sources are placed on the object in order to measure the times of flight (ToF) and distances between them and the microphones, connecting the array and the object together. The overall geometric configuration is thus defined by an Euclidean Distance Matrix (EDM), which is basically the matrix of squared distances between points. First, Multidimensional Scaling (MDS) technique is used to reconstruct the point set from distances. Second, this point set is then aligned with the sources whose coordinates are known. This orthogonal Procrustes problem is solved by the Kabsch algorithm to obtain the rotation and translation matrices between the coordinate system of the array and the object of study. In addition, a low rank property of Euclidean distance matrices is exploited to evaluate *in situ* the speed of sound. The main theoretical and algorithmic elements are exposed and a numerical simulation of a geometric configuration, representative of a typical experimental set-up, is carried out. The robustness of the method is finally discussed.

PACS no. 43.60.Fg

1. Introduction

The localization and quantification of acoustic sources radiated by a device depend on numerous physical parameters as well as the choice of measurement array of microphones or the back-propagating method. As highlighted recently by Gilquin *et al.* [1] by means of sensitivity analysis, deviations of the antenna position and orientation in its experimental environment influence greatly the sound source reconstruction, both with a classical beamforming technique or a Bayesian formulation.

The antenna positioning problem is illustrated in Figs. (1) and (2) : one array of microphones is facing towards a device (here a basic mock-up of an

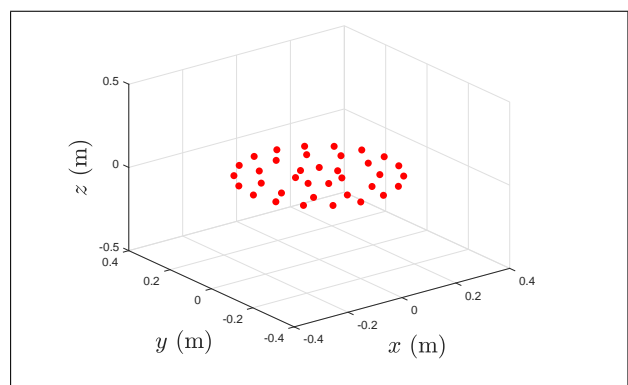


Figure 1. Position of microphones (red dots) in the array coordinate system.

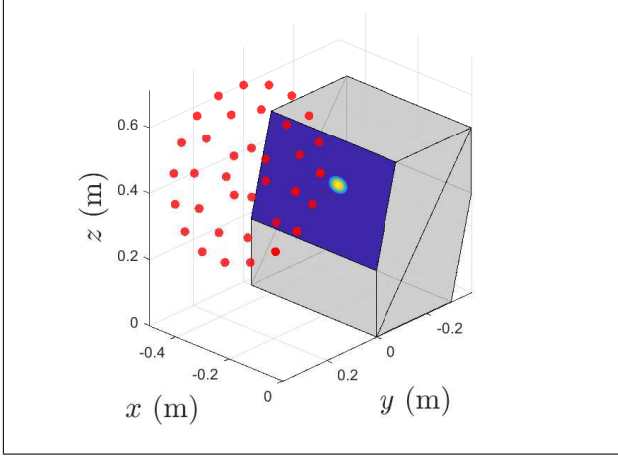


Figure 2. Position of the antenna (red dots) in the device coordinate system (ground truth). The array of microphones faces towards a radiating surface to reconstruct.

pletely known. A mesh of the surface of interest is achieved to retro-propagate the acoustic field measured by the array on the device. Several methodologies have been proposed to determine the true position of each sensor in a network, especially through microphone position self-calibration [2]. The aim of this study is rather to determine the antenna position in relation to the device during an experimental campaign and collect each microphone coordinates in the mesh coordinate system to perform the back-propagation. This application-oriented paper gathers different techniques based on Euclidean distance geometry to develop a practical tool. The theoretical and algorithmic elements of these methods are detailed and illustrated all along the study with the same numerical simulation, representative of a typical experimental set-up. Section (2) first details how to define the overall geometric configuration with the Euclidean distance matrix (EDM) and complete it with the help of a set of acoustic sources placed on the device. The point set is then reconstructed from the distances with a multidimensional scaling technique, presented in Section (3). The set is then aligned with the collection of sources, defined as anchors to provide the rigid transformation between the coordinate system of the array and the device, with the help of the Kabsch algorithm (Section (4)). Finally, Section (5) proposes a low-rank based criterion to experimentally evaluate the speed of sound, whose knowledge is needed in the proposed method.

2. Euclidean Distance Matrix

2.1. Properties

Consider a d -dimensional Euclidean space, where n points are set and described by the columns of the matrix $\mathbf{X} \in \mathbb{R}^{d \times n}$, $\mathbf{X} = [\mathbf{x}_1, \mathbf{x}_2, \dots, \mathbf{x}_n]$, $\mathbf{x}_i \in \mathbb{R}^d$. The terms d_{ij} of an Euclidean distance matrix $\mathbf{D} \in$

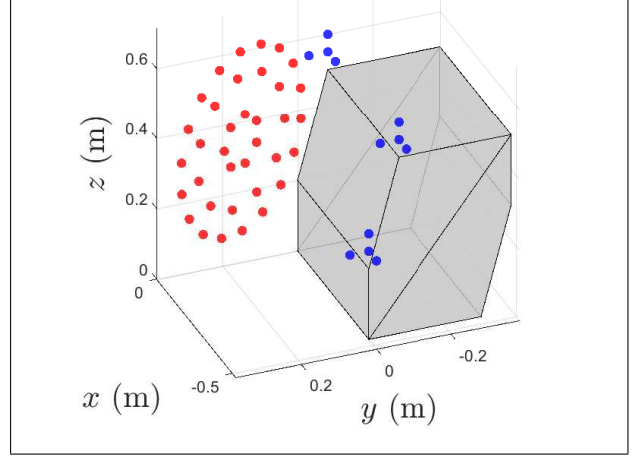


Figure 3. Ground truth of the antenna positioning problem. Microphones are represented by red dots while blue dots depict acoustic sources.

$\mathbb{R}^{n \times n}$ are the squared distances between points \mathbf{x}_i and \mathbf{x}_j :

$$d_{ij} = \|\mathbf{x}_i - \mathbf{x}_j\|_2^2, \quad (1)$$

where $\|\cdot\|_2$ is the Euclidean norm. An EDM fulfills the following properties :

- Non-negativity ($d_{ij} \geq 0$, $i \neq j$)
- Hollow matrix ($d_{ij} = 0 \Leftrightarrow i = j$)
- Symmetry : $d_{ij} = d_{ji}$

Furthermore, as shown by Gower [3], the rank of an EDM \mathbf{D} related to the set of points \mathbf{X} satisfies the inequality :

$$\text{rank}(\mathbf{D}) \geq d + 2. \quad (2)$$

The Euclidean distance matrix is also invariant under orthogonal and rigid transformations (such as rotation, reflection and translation). As a consequence, the absolute position and orientation of a point set cannot be reconstructed from the associated EDM. Each result is then a rigid transformation of another one. For more details, Parhizkar [4] provides a complete description of the EDM algebra.

2.2. Constructing the EDM

Figure (3) illustrates the ground truth of the antenna positioning problem, as met in an experimental campaign. The coordinates of each microphone (red dots) in the array system are known, as the distances between them. Acoustic sources (blue dots) are placed at some prominent locations of the device. They are gathered in a group of four by a structural support (Fig. (4)), which is moved to each location. This support allows increasing the number of sources (and hence the EDM size) while limiting the number of measurement points. The position of these reference

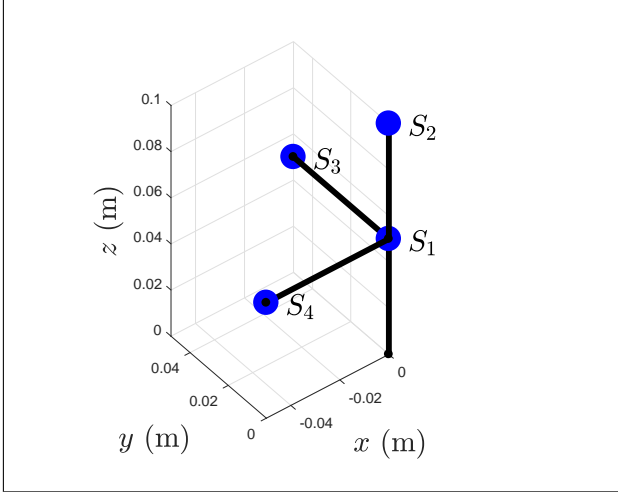


Figure 4. Structural support of the four acoustic sources (blue dots). At the origin is a fulcrum (small black dot), in contact with a prominent location of the device.

points and the acoustic sources are known in the device coordinate system.

At the initializing step of the method, some submatrices of the EDM are already known (Fig. (5)) : the diagonal block submatrices related to microphones (top-left block) and to sources (bottom-right block). The size of each block is the number of microphones or sources, respectively. The distances between microphones and sources, represented by the blank off-diagonal submatrices are unknown.

The determination of the distance between a source and microphone is based on time of flight (ToF) measurements. This time of propagation between the two points is obtained by cross-correlating the microphone signal with a sound emitted by the synchronized reference source. The benefit of the synchronization is the possibility to select the first peak of cross-correlation related to the straight path, avoiding reflection issues due to the proximity between the array and the device. An evaluation of the speed of sound is finally needed to calculate the distance from the time of flight. The sound of reference sources is chosen according to the quality of the cross-correlation measurements. Each source can simultaneously emits uncorrelated white noise or modulated sweep sines. In the numerical simulation, the same linear chirp is sequentially emitted by each source. The frequency linearly increases from 0 to 10 kHz and the sampling frequency is 50 kHz. The speed of sound is set at 343 m/s. As the peak detection depends on the length of the time sample, the sampling frequency is an essential parameter. At a fixed sampling frequency f_s , the maximum error on distance Δd induced by the sampling is $\Delta d = c_0/f_s$. At $f_s = 50$ kHz, Δd is theoretically smaller than 7 mm. In the simulation, the reconstruction error on the distance between sources and microphones due to this sampling issue does not

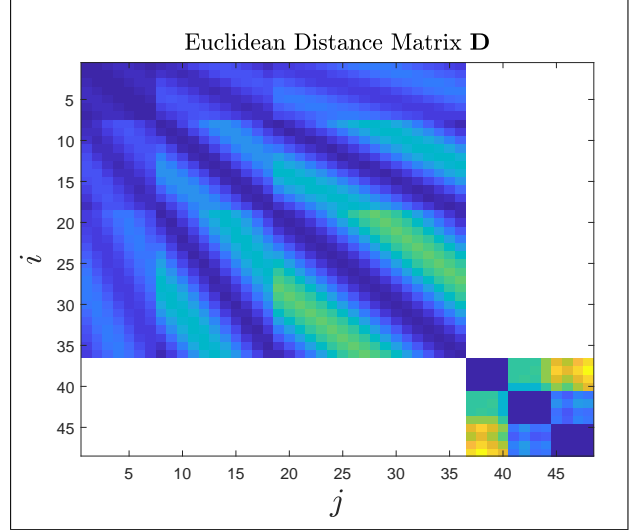


Figure 5. Incomplete Euclidean distance matrix. The diagonal block submatrices represent distances between microphones (top-left block) and sources (bottom-right block), while distances between microphones and sources are unknown (blank off-diagonal submatrices). i and j denote the index of a particular point in the set-up.

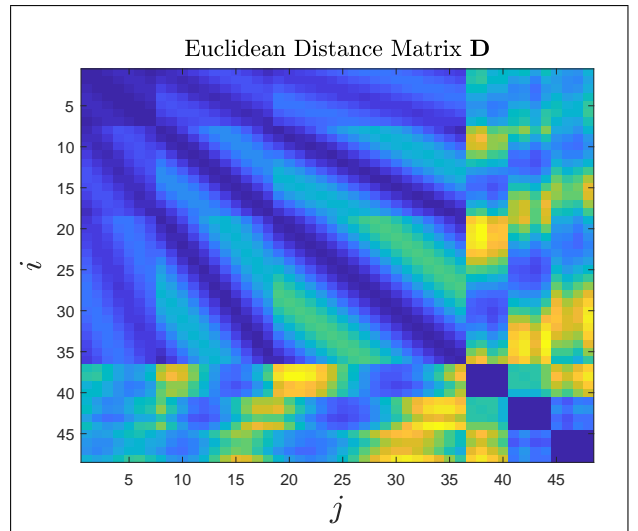


Figure 6. Completed Euclidean distance matrix.

exceed 3.5 mm. Finally, Fig. (6) illustrates the completed EDM.

3. Multidimensional Scaling

Multidimensional scaling (MDS) refers to a collection of techniques for the analysis of similarity or dissimilarity in a dataset. Initially developed in psychometrics [5], MDS allows modeling a wide range of data as distances and visualizing them as points in a geometric space. The algorithm 1 presents the classical MDS, also known as Torgerson-Gower scaling [6], which finds a coordinate matrix $\tilde{\mathbf{X}}$ starting from an EDM \mathbf{D} and the embedded dimension d .

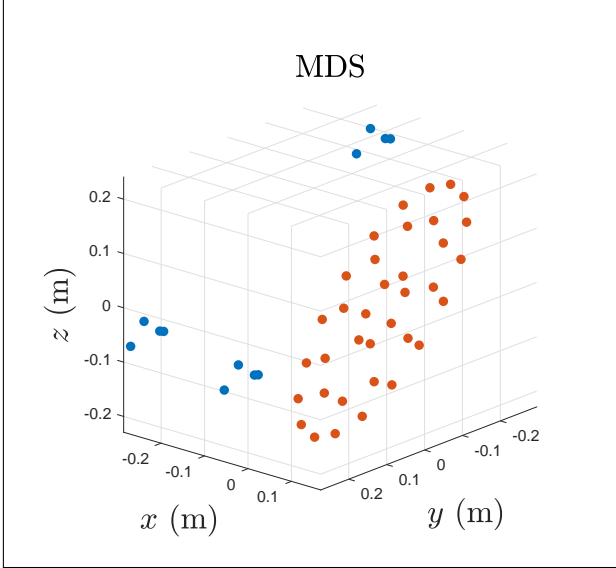


Figure 7. Multidimensional scaling of the numerical set-up. The blue and red dots represent the sources and the microphones, respectively.

The mathematical developments are detailed by Dokmanić *et al.* [7] and Borg and Groenen [6].

Algorithm 1 ClassicalMDS(\mathbf{D} , d), [7]

Require: \mathbf{D} , d

- 1: $\mathbf{J}(n) = \mathbf{I} - \frac{1}{n} \mathbf{1}\mathbf{1}^T$ \triangleright Geometric centering matrix
 - 2: $\mathbf{G} = -(1/2)^n \mathbf{J}\mathbf{D}\mathbf{J}$ \triangleright Gram matrix
 - 3: \mathbf{U} , $\mathbf{\Lambda} \leftarrow \text{EVD}(\mathbf{G})$ \triangleright Eigendecomposition
 - 4: **return** $\hat{\mathbf{X}} = [\text{diag}(\sqrt{\lambda_1}, \dots, \sqrt{\lambda_d}, \mathbf{0}_{d \times (n-d)})] \mathbf{U}^T$
-

The method is based on an eigendecomposition of the Gram matrix ($\mathbf{G} = \mathbf{X}^T \mathbf{X}$, where $(\bullet)^T$ denotes the transpose operator). According to Gower [8], this matrix can be computed with a double centering, using the geometric centering matrix \mathbf{J} , where $\mathbf{1}$ is a column vector filled with ones. The eigenvalues λ_i are sorted in order of decreasing amplitude and only the d first values are selected. Thus, the point set $\hat{\mathbf{X}}$ is embedded in a d -dimensional space.

Figure (7) shows a multidimensional scaling of the numerical set-up. As it can be seen, the position and orientation of the overall geometric configuration are completely arbitrary, and more, the MDS result is actually a reflection of the true set-up.

4. Orthogonal Procrustes Analysis

As explained in Section (2.1), the EDM is invariant under orthogonal and rigid transformations. Therefore, the absolute orientation and position of the point

set cannot be derived from the multidimensional scaling. A secondary step is needed to find the optimal rotation/reflection and translation matrices which align the point set in the reference frame of the device. This is performed with a selection of n_s points, denoted as anchors, whose positions \mathbf{X}_s in this particular coordinate system are known. This step is usually called orthogonal Procrustes analysis [9]. One solution, stemmed from crystallography, is the Kabsch algorithm [10, 11], which computes the optimal rotation matrix \mathbf{R} between two sets of points by minimizing the root mean square deviation (least RMSD, Eq. (3)).

$$\text{IRMSD} = \underset{\mathbf{R} \in \mathbb{R}^{d \times d}}{\text{argmin}} \sqrt{\frac{1}{n_s} \sum_{i \in n_s} |\mathbf{R} \hat{\mathbf{x}}_{s,i} - \mathbf{x}_{s,i}|^2}. \quad (3)$$

First of all, the two set of anchors in both reference frames (MDS, $\hat{\mathbf{X}}_s$ and device, \mathbf{X}_s) must be translated to align their centroid with the origin of the coordinate system. The Kabsch algorithm is then based on a singular-value decomposition (SVD) of the cross-covariance matrix $\hat{\mathbf{X}}_s \mathbf{X}_s^T$:

$$\mathbf{U}[\mathbf{S}]\mathbf{V}^H = \hat{\mathbf{X}}_s \mathbf{X}_s^T \quad (4)$$

where $(\bullet)^H$ denotes the Hermitian transpose operator and $[\bullet]$ a diagonal matrix. The optimal rotation matrix reads :

$$\mathbf{R} = \mathbf{V} \begin{pmatrix} 1 & 0 & 0 \\ 0 & 1 & 0 \\ 0 & 0 & d_c \end{pmatrix} \mathbf{U}^H, \quad d_c \in \{-1, 1\}. \quad (5)$$

If $d_c = 1$, the two matrices $\hat{\mathbf{X}}_s \mathbf{R} + \mathbf{T}$ and \mathbf{X}_s are identical whereas one of the matrices is the reflection of the other if $d_c = -1$. All those steps are summarized in Algorithm 2.

Algorithm 2 Kabsch($\hat{\mathbf{X}}_s$, \mathbf{X}_s , d , n_s)

Require: $\hat{\mathbf{X}}_s$, \mathbf{X}_s , d , n_s

- 1: $\hat{\mathbf{X}}_s = \mathbf{J}(n_s) \hat{\mathbf{X}}_s$ \triangleright align centroid with origin
 - 2: $\mathbf{X}_s = \mathbf{J}(n_s) \mathbf{X}_s$ \triangleright align centroid with origin
 - 3: $\mathbf{C} = \hat{\mathbf{X}}_s \mathbf{X}_s^T$ \triangleright Cross-covariance matrix
 - 4: $\mathbf{U}[\mathbf{S}]\mathbf{V}^H = \mathbf{C}$ \triangleright SVD
 - 5: **return** $\mathbf{R} = \mathbf{V}\mathbf{U}^H$ \triangleright Rotation matrix
 - 6: **return** $\mathbf{T} = \mathbf{X}_{s,c} - \mathbf{R}\hat{\mathbf{X}}_{s,c}$ \triangleright Translation vector
 - 7: **return** IRMSD \triangleright least root mean square deviation
-

The Kabsch algorithm is then applied to the numerical set-up. More specifically, this method is carried on to find the optimal rotation matrix between the position of sources obtained by the MDS and their exact position in the device coordinate system. Figure (8) shows the final result of the complete

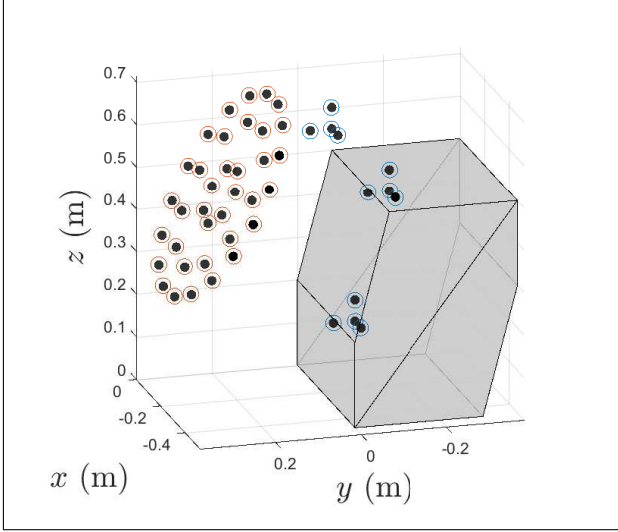


Figure 8. Final result of the positioning algorithm. The black dots, the blue and red circles represent the ground truth position and the estimated position of the sources and microphones, respectively.

methodology detailed in this paper. It roughly shows that the array is aligned with the ground truth (black dots). The red and blue dots represent the estimated positions of microphones and sources, respectively. If required, the algorithm can be performed a second time, taking the position of the microphones in the array and device coordinate systems as inputs. This new step provides directly the rigid transformation between the coordinate system of the array and the device.

A positioning error Δ is calculated, based on the distances between the true positions of microphones and sources (ground truth, \mathbf{X}), and those estimated by the positioning method ($\hat{\mathbf{X}}$). For a microphone of the array (a) or a source (s), the residue reads :

$$\Delta_{a,s} = \|\hat{\mathbf{X}}_{a,s} - \mathbf{X}_{a,s}\|_2^2. \quad (6)$$

As shown by Figs (9) and (10), the maximum errors of reconstruction are 1.46 and 3.12 mm for the sources and microphones, respectively. Those errors come to a great extent from the sampling issue detailed in Section (2.2).

5. In Situ Evaluation of Sound Speed

As shown by Eq.(2), the rank of an EDM is at least equal to $d + 2$, where d is the spatial dimension of the geometric configuration. This section introduces a simple criterion built on this specific property to estimate the experimental value of the speed of sound. As seen in Section (2.2), evaluating the source-microphone distances requires both an accurate estimation of the times of flight and the speed of

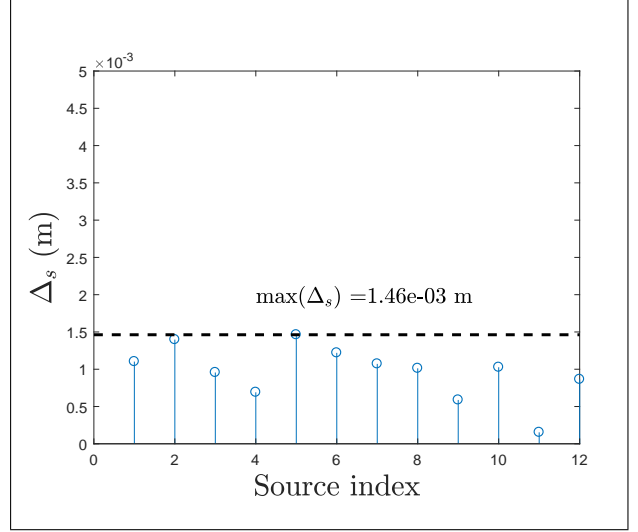


Figure 9. Source positioning error Δ_s according the source index.

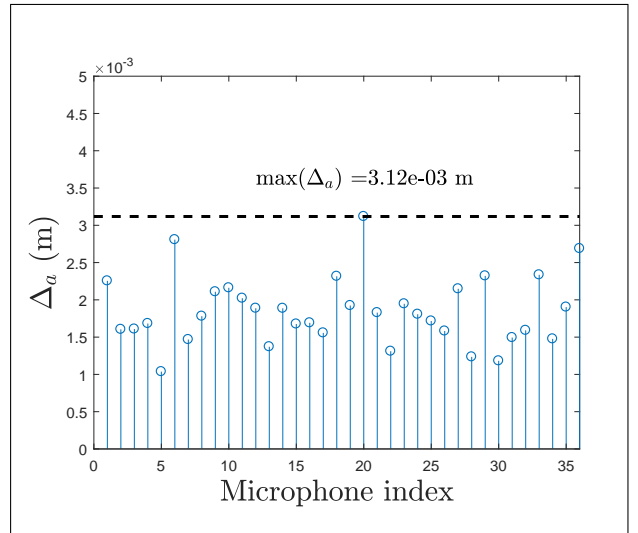


Figure 10. Microphone positioning error Δ_a according the microphone index.

sound. Thus, the latter is involved in the off-diagonal submatrices of the EDM. The low-rank property implies the first $d + 2$ singular values s_i of the Euclidean distance matrix overwhelm the others. The criterion Λ_{c_0} (Eq.(7)) estimates the information brought by the smaller singular values in the total amount of energy contained in the matrix. Minimizing Λ_{c_0} with respect to c_0 ensures the Euclidean nature of the geometry, avoiding any curvature effect.

$$\Lambda_{c_0} = \frac{\sum_{i>d+2} s_i}{\sum_{i \in \mathbb{N}} s_i}, \quad s_i \triangleq \mathbf{S}(i, i). \quad (7)$$

Figure (11) illustrates the estimation of the speed of sound. c_0 is set at 343 m/s in the simulation and the sampling frequency of the propagating signals is 50 kHz. A range of possible values is swept

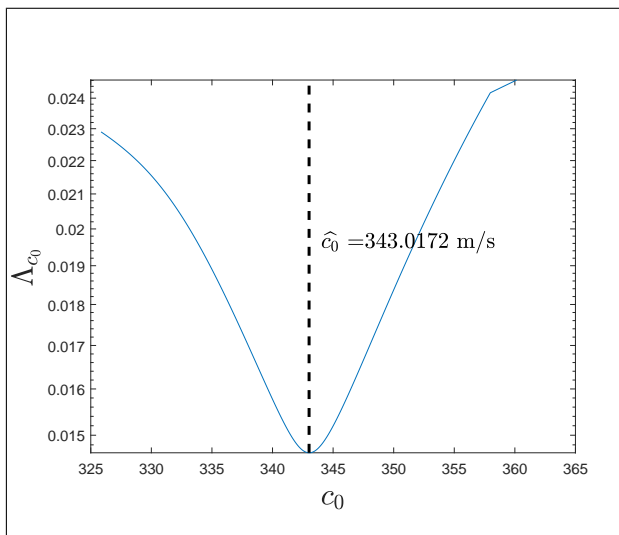


Figure 11. Evaluation of the experimental speed of sound \hat{c}_0 .

($c_0 \in [325, 365]$ m/s) and the criterion Λ_{c_0} reaches a unique and well-defined minimum. The optimal speed of sound \hat{c}_0 is then equal to 343.017 m/s.

6. Conclusions

An array localization technique has been detailed in this paper. It gathers a collection of methods based on Euclidean distance geometry. The main theoretical element is the Euclidean distance matrix, which reports on the geometric configuration of a set-up. Acoustic sources, placed on several locations of the device, act as anchors to connect the antenna of microphones to it. As the EDM deals with pairwise distances between points, these sources have to be visible from the microphones. In addition, as the EDM is invariant under orthogonal transformation, especially reflection, the anchors positions must form an asymmetrical configuration in a three-dimensional space. Once the anchors are set and their positions known in the device coordinate system, the source-microphone distances are calculated to complete the EDM. The time of propagation between the two points is obtained by cross-correlating the microphone signal with a calibration sound emitted by the synchronized source. The sampling of the signal involves a limit on the resolution of the first peak, representing the straight path between the source and the microphone. The sampling frequency is therefore an influent parameter on the distance estimation and the global reconstruction error. Once the EDM is complete, the positioning problem is solved using a multidimensional scaling technique and a Kabsch algorithm to find the optimal rotation and translation matrices to align the array with its ground truth position. The results show a good agreement between the estimated position of the array and the ground

truth, with a maximum positioning error around 3 mm. Finally, a low-rank property of the EDM is exploited to evaluate the experimental speed of sound.

This method allows one to easily get the position of an array in regards to the object of study during an experimental campaign. Its advantage is that it can benefit from extensions provided by the EDM literature to tackle many issues faced in domains of source localization and acoustic array processing.

Acknowledgement

This study has been produced in the framework of LUG2 supported by Région Auvergne Rhône-Alpes and BPIFrance (FUI22). It was performed within the framework of the Labex CeLyA of Université de Lyon, operated by the French National Research Agency (ANR-10-LABX-0060/ANR-11-IDEX-0007).

References

- [1] Laurent Gilquin, Simon Bouley, Jérôme Antoni, Clément Marteau, and Thibaut Le Magueresse. Sensitivity analysis of acoustic inverse problems. In *Proceedings of NOVEL 2018, Ibiza, Spain*, 2018.
- [2] Axel Plinge, Florian Jacob, Reinhold Haeb-Umbach, and Gernot A. Fink. Acoustic microphone geometry calibration: An overview and experimental evaluation of state-of-the-art algorithms. *IEEE Signal Processing Magazine*, 33(4):14–29, 2016.
- [3] John C. Gower. Properties of euclidean and non-euclidean distance matrices. *Linear Algebra and its Applications*, 67, 1985.
- [4] Reza Parhizkar. *Euclidean distance matrices: Properties, algorithms and applications*. PhD thesis, École Polytechnique Fédérale de Lausanne (EPFL), 2013.
- [5] Warren S. Torgerson. Multidimensional scaling: I. theory and method. *Psychometrika*, 17(4):401–419, 1952.
- [6] Ingwer Borg and Patrick J. Groenen. *Modern multidimensional scaling: Theory and applications*. Springer-Verlag New York, 2 edition, 2005.
- [7] Ivan Dokmanić, Reza Parhizkar, Juri Ranieri, and Martin Vetterli. Euclidean distance matrices: essential theory, algorithms, and applications. *IEEE Signal Processing Magazine*, 32(6):12–30, 2015.
- [8] John C. Gower. Euclidean distance geometry. *Math. Sci*, 7(1):1–14, 1982.
- [9] John C. Gower. Procrustes methods. *Wiley Interdisciplinary Reviews: Computational Statistics*, 2(4):503–508, 2010.
- [10] Wolfgang Kabsch. A solution for the best rotation to relate two sets of vectors. *Acta Crystallographica Section A: Crystal Physics, Diffraction, Theoretical and General Crystallography*, 32(5):922–923, 1976.
- [11] Wolfgang Kabsch. A discussion of the solution for the best rotation to relate two sets of vectors. *Acta Crystallographica Section A: Crystal Physics, Diffraction, Theoretical and General Crystallography*, 34(5):827–828, 1978.